Electrochemistry Communications 87 (2018) 31–34

Contents lists available at ScienceDirect

Electrochemistry Communications

journal homepage: www.elsevier.com/locate/elecom

In-situ electronic conductivity measurements of $LiNi_{0.45}Mn_{1.485}Cr_{0.05}O_4$ thin films using all-solid-state thin-film batteries

Morihiro Sato, Takayuki Yamamoto, Munekazu Motoyama, Yasutoshi Iriyama*

Department of Materials Design Innovation Engineering, Graduate School of Engineering, Nagoya University, Furo-cho, Chikusa-ku, Nagoya 4648603, Japan

ARTICLE INFO

Keywords:
All-solid-state rechargeable lithium battery
Electronic conductivity
Grain boundary

ABSTRACT

Total electronic conductivity (σ_e^{total}) of $LiNi_{0.45}Mn_{1.485}Cr_{0.05}O_4$ thin film (LNM–Cr: 40 nm in thickness) between 3.5 and 4.9 V (vs. Li metal anode) was measured using all-solid-state thin-film battery (Li/LiPON/LPO/LNM–Cr) fabricated on interdigitated array (IDA) electrode. The LNM–Cr with disordered spinel phase was prepared by pulsed laser deposition on the IDA electrode. The σ_e^{total} depended on the voltage and reversibly changed regardless of lithium extraction/insertion process. Variation trends of the σ_e^{total} were in good agreement with the previous reports using the chemically delithiated powder materials. Grain boundary resistance contributes to the σ_e^{total} depending on the voltage probably because of the formation of double Schottky barrier at the grain boundaries.

1. Introduction

5 V-class electrode active materials have received much attention to develop advanced rechargeable lithium batteries with higher energy density [1–3]. Among them, $LiNi_{0.5}Mn_{1.5}O_4$ (LNM) is composed of cheap and abundant transition metals of Ni and Mn, and their electrochemical properties have been investigated extensively [4–7]. Variations of total electronic conductivity (σ_e^{total}) of the LNM have been reported using chemically delithiated powder materials [8]. To investigate the σ_e^{total} by electrochemically lithium inserted/extracted materials, usage of thin-film electrodes is a powerful method because they can operate without conductive additives and binders [9]. Although operation of the LNM at 5 V region has problems in conventional organic liquid electrolytes such as electrode dissolution and electrolyte decomposition on the electrode surface, these problems are avoided by using all-solid-state thin-film battery (TFB) technology.

Here, we prepared Cr-doped LNM thin films (LNM–Cr) by pulsed laser deposition (PLD) on interdigitated array (IDA) electrodes and developed TFBs. Lithium insertion/extraction reactions of the LNM–Cr were carried out on the IDA electrodes and the σ_e^{total} was measured at a given voltage between 3.5 and 4.9 V (vs. Li metal anode).

2. Experimental

The LNM–Cr with the composition of $LiNi_{0.45}Mn_{1.485}Cr_{0.05}O_4$ were prepared on IDA electrodes at 700 °C by PLD which guarantee stable reactions [4]. Base material of the IDA electrodes were SiO_2 ($12 \times 20\ mm^2$) on which both IDA electrodes (W1 and W2) and another electrodes (counter electrode (CE) and reference electrode (RE)) made of thin–film Pt were printed (BAS Inc. [10]). Schematic image of the IDA electrode is shown in Fig. 1(a). The number of paired array (n) was 129, and each array with the length (a (μm)) of 2.0×10^3 μm was separated with the distance (L (μm)) of 3.0 μm. The LNM–Cr with the thickness (h (μm)) of 0.04 μm was deposited on the IDA electrode by using physical mask as shown by blue-squared region in Fig. 1(a). Electronic resistance (R (Ω)) of the LNM–Cr was measured between W1 and W2, and the σ_e^{total} (S cm^{-1}) was calculated from below equation.

$$\sigma_e^{total} = \frac{10000\ L}{R \times h \times a \times n} \quad (1)$$

Thin film of amorphous lithium phosphate (LPO: 0.1 μm in thickness) was deposited at first on the LNM–Cr by PLD to reduce the charge transfer resistance (~10 Ω cm^2) (orange square region in Fig. 1(a)) probably by negligible space charge effect in addition to damage-less interface [11–13]. After that, thin film of lithium phosphorus oxynitride glass electrolyte (LiPON: 5 μm in thickness) was deposited on the LPO by RF magnetron sputtering (orange square region in Fig. 1(a)) [14], and then lithium metal film (Li: 2 μm in thickness) was deposited on the LiPON film by vacuum deposition so as to be electronically connected to CE and RE (gray square region in Fig. 1(a)) also by using physical masks. Usage of thick LiPON film formation was to eliminate the possibilities of short circuits during the fabrication of TFB. Cross-sectional SEM image of the resultant TFB (Li/LiPON/LPO/LNM–Cr) are displayed in Fig. 1(b).

* Corresponding author.
E-mail address: iriyama@numse.nagoya-u.ac.jp (Y. Iriyama).

https://doi.org/10.1016/j.elecom.2017.12.021
Received 20 November 2017; Received in revised form 18 December 2017; Accepted 19 December 2017
Available online 23 December 2017
1388-2481/

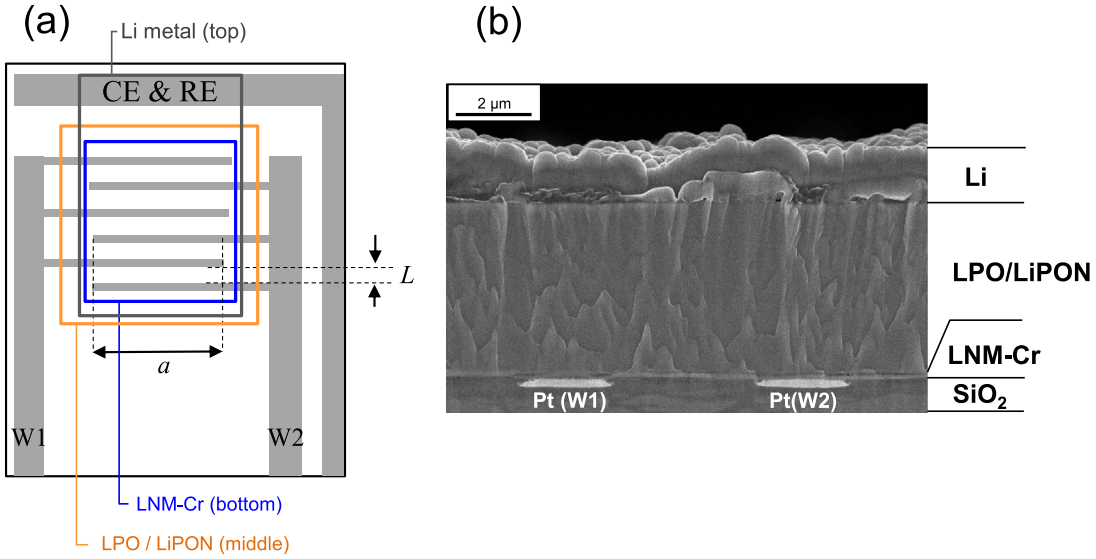

Fig. 1. Schematic top-view image of a TFB formed on an IDA electrode. Thin films of LNM–Cr, LPO/LiPON, and Li were sequentially deposited in the blue, orange, and gray square regions, respectively. (b) Cross–sectional SEM image of a TFB. (For interpretation of the references to color in this figure legend, the reader is referred to the web version of this article.)

Electrochemical lithium insertion/extraction reactions of the LNM–Cr were measured using the TFB by cyclic voltammetry (CV), where both W1 and W2 are connected to be single working electrode. The σ_e^{total} at a given voltage was measured as follows. The TFB was charged or discharged to a voltage by linear sweep voltammetry, and the TFB was maintained at the voltage until the residual current decreased less than 0.1 μA. After that, both the W1 and the W2 were disconnected from CE and RE and were separated each other. Then, symmetrical electronically non-blocking two electrodes system, Pt (W1)/LNM–Cr/Pt(W2), was formed on the IDA electrodes to measure the *R* of the LNM–Cr at a given voltage. Each *R* was measured at 25 °C by A.C. impedance spectroscopy with a frequency range of 200 kHz-100 MHz at an A.C. amplitude of 10 mV in an Ar-filled grove box. We have checked that ion conductive circuit (for example, LPO/LiPON/LPO) and another possible electron transfer circuit (for example, LPO/LiPON/Li/LiPON/LPO) do not contribute to the *R*. The ZView program (Scribner associates Inc.) was used to calculate the capacitance and for curve fitting.

3. Results and discussion

Fig. 2(a) shows SEM images of the LNM–Cr deposited on an IDA electrode. We checked uniform distribution of Ni, Mn, and Cr by surface EDX analysis as shown in the insets of Fig. 2(a). The magnified SEM image in dotted rectangular region indicates that the LNM–Cr is made of small crystallite with ca. 100 nm in diameter and has many grain boundaries.

Fig. 2(b) shows the XRD patterns of the LNM–Cr and an IDA electrode annealed at 700 °C. The diffraction peak marked by * originates from Pt films of the IDA electrode and then the diffraction peak at 18.5° is indexed to 111 reflection of the LNM–Cr, suggesting the formation of crystalline film. Fig. 2(c) shows the Raman spectrum of the LNM–Cr. The LNM favors two kinds of phases, so–called ordered spinel with $P4_332$ symmetry and disordered spinel with $Fd\bar{3}m$ symmetry [6]. The ordered LNM has characteristic Raman bands at 166, 221, and 241 cm^{-1} in addition to the peak separation of F_{2g} around 600 cm^{-1} [15,16]. Because those peaks were not observed at all in Fig. 2(c), we can conclude that the LNM–Cr forms the disordered spinel phase. Slight doping of Cr in the LNM may facilitate the disordered spinel phase [17]. Fig. 2(d) shows the Nyquist plots of the LNM–Cr. Only one semicircular arc was observed due to the electronic conduction in the LNM–Cr. The *R* of the LNM–Cr were estimated from the diameter of the semicircular arc, and the σ_e^{total} was calculated from Eq. (1) to be 9.7×10^{-5} S cm^{-1}. This value is in good agreement with the previous report [8], and we can conclude that σ_e^{total} of the LNM–Cr is measured well by the IDA electrode.

Fig. 3(a) shows the CV of the TFB between 3.5 and 4.9 V at 0.5 mV s^{-1}, where the starting voltage was 3.5 V. Typical redox peaks of the LNM due to $Mn^{3+/4+}$ around 4.0 V (but not two couples of redox peaks typically observed for $LiMn_2O_4$) and $Ni^{2+/3+/4+}$ around 4.7 V were observed. The CV measurements were repeated several times to check the stability as with our past report [4]. The σ_e^{total} was measured alpha-numerically, from 1 to 11. One or two semicircles were observed in each Nyquist plot measured at each numbered voltage as displayed in Fig. 3(b). The capacity of the semicircle observed at higher frequency was almost constant ($0.8 - 1.2 \times 10^{-10}$ F), while that of the semicircle observed at lower frequency varied in $0.1 - 7.7 \times 10^{-5}$ F. The higher-frequency semicircle will be assigned to in-grain resistance (R_{ig}), and the lower-frequency one to grain boundary resistance (R_{gb}) [8]. The equivalent circuit model is shown in the inset of Fig. 3(b) at 3.5 V. Each σ_e^{total} at a given voltage was measured from the total resistance, $R_{ig} + R_{gb}$, and the variations of the σ_e^{total} are plotted in Fig. 3(a). Each R_{gb} in the spectra of No. 2, 3, 9, 10, and 11 were estimated by a curve fitting. The σ_e^{total} at 3.5 V was 8.7×10^{-5} S cm^{-1} (No. 1), which decreased to 9.3×10^{-6} S cm^{-1} (No. 3) after the oxidation peak of $Mn^{3+/4+}$ at 4.0 V. This abrupt drop has been explained by the consumption of conductive active Mn^{3+} due to lithium extraction from the LNM [8]. After 4.5 V, the σ_e^{total} increased to $5.0 - 6.2 \times 10^{-4}$ S cm^{-1} (No.4–6) in the easier carrier conduction region in the Ni: 3*d* band ($Ni^{2+/3+}$ and $Ni^{3+/4+}$ redox region). Slight smaller values of the σ_e^{total} over 4.7 V than those of chemically delithiated LNM are probably because conductive Ni was partially exchanged with Cr. The σ_e^{total} showed almost same value even at the electrochemical lithium insertion process (No. 7–11), indicating the σ_e^{total} changes reversibly between 3.5 and 4.9 V regardless of lithium insertion/extraction process. Variation trends of the σ_e^{total} were in good agreement with the past report using the chemically delithiated powder samples [8].

It should be noted that the R_{gb} contributes to the total resistance depending on the voltage and that the R_{gb} is not observed over 4.7 V. The volume of the LNM shrinks at higher voltage (~6.5%) [8], and then the disappearance of the R_{gb} over 4.7 V is not explained from geometrical contact area loss at grain boundaries. Also, the R_{gb} was not observed in the as-prepared LNM–Cr but the R_{gb} appeared in the TFB (No. 1 (3.5 V) in Fig. 3(a)) after the charge-discharge reactions. During